



Contents lists available at ScienceDirect

Chemical Engineering Journal

journal homepage: www.elsevier.com/locate/cej

Three step synthesis of benzylacetone and 4-(4-methoxyphenyl)butan-2-one in flow using micropacked bed reactors

Conor Waldron^a, Enhong Cao^a, Stefano Cattaneo^b, Gemma L. Brett^b, Peter J. Miedziak^b, Gaowei Wu^a, Meenakshisundaram Sankar^b, Graham J. Hutchings^b, Asterios Gavriilidis^{a,*}

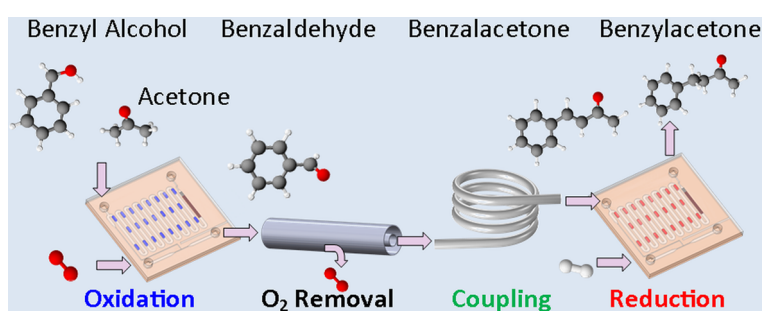
^a Department of Chemical Engineering, University College London, London WC1E 7JE, UK

^b Cardiff Catalysis Institute, School of Chemistry, Cardiff University, Cardiff CF10 3AT, UK

HIGHLIGHTS

- Three catalytic reactors and a separator were combined in a telescoped flow system.
- Telescoped flow synthesis allowed different operating conditions for each reaction.
- Telescoped flow achieved higher yields than batch for production of ketones.

GRAPHICAL ABSTRACT



ARTICLE INFO

Keywords:

Telescoped synthesis
Cascade synthesis
Catalytic microreactor
Oxidation
Hydrogenation
Coupling

ABSTRACT

The synthesis of benzylacetone from benzyl alcohol and of 4-(4-methoxyphenyl)butan-2-one from 4-methoxybenzyl alcohol, which were previously performed in a batch cascade, were successfully performed in a telescoped flow system consisting of three micropacked bed reactors and a tube-in-tube membrane to remove oxygen. The system consisted of approximately 10 mg of 1 wt% AuPd/TiO₂ catalyst for oxidation, 150–250 mg of anatase TiO₂ for C–C coupling and 10 mg of 1 wt% Pt/TiO₂ for reduction, operating at 115 °C, 130 °C and 120 °C respectively. Oxygen and hydrogen flowrates were 2 and 1.5 NmL/min and alcohol solution inlet flowrates were 10–80 μL/min, while the system operated at a back pressure of 5 barg. This system achieved significantly increased yields of benzylacetone compared to the batch cascade (56% compared to 8%) and slightly increased yields of 4-(4-methoxyphenyl)butan-2-one (48% compared to 41% when using the same catalyst supports). The major advantage of the telescoped flow system was the ability to separate the three reactions, so that each reaction could have its own catalyst and operating conditions, which led to significant process intensification.

1. Introduction

Over the last decade there has been a significant increase in both the number and complexity of telescoped flow synthesis, where flow reactors and separator systems are connected together in series to enable the synthesis of complex products. A large number of telescoped

reactions have already been reported in the literature in a range of research areas including active pharmaceutical ingredient (API) synthesis [1–9], biofuels [10–12] and the fine chemicals industry [13–18]. These telescoped systems offer many opportunities for process intensification due to the inherent advantages of flow reactors including increased rates of heat and mass transport, access to a wider

* Corresponding author.

E-mail address: a.gavriilidis@ucl.ac.uk (A. Gavriilidis).

<https://doi.org/10.1016/j.cej.2018.09.137>

1385-8947/ © 2018 The Authors. Published by Elsevier B.V. This is an open access article under the CC BY license (<http://creativecommons.org/licenses/by/4.0/>).

Please cite this article as: Waldron, C., Chemical Engineering Journal, <https://doi.org/10.1016/j.cej.2018.09.137>

range of reaction conditions, increased safety and improved control of reaction conditions [19–22]. This recent progress in telescoped systems has largely been enabled by developments in continuous flow downstream processing unit operations, such as liquid-liquid separation [23,24], extraction [18], gas-liquid separation [25] and crystallisation [1], as well as by developments in automation allowing easier control of complicated systems [26].

Despite the considerable progress made in telescoped systems, there are still challenges to be overcome, one of the most important being solid handling, including both solids formed during reaction and solids added to the reactor [27]. In flow reactors, pumping solids in slurries is difficult, especially for microreactors, and can often lead to reactor clogging and blockages making systems unreliable and preventing prolonged continuous operation [26]. While there are various solutions for lab scale slurry reactors including the use of sonication [28,29], agitation [30], droplet flow [31], gas-liquid slug flow [32] or specially designed reactors including cascade of CSTRs [33–35], these solutions increase system complexity. Furthermore, many of these solutions require the slurry to flow into and out of the reactor [28–35] instead of being retained in the reactor, which may be required in a telescoped flow system if it is desired to use different slurry catalysts in sequential reactors. Retaining the slurry in the reactor is more difficult as it requires filtration before the reactor outlet, leading to problems with clogging. For this reason most telescoped systems which require solid catalysts avoid slurry reactors and instead rely on fixed bed reactors where the catalyst is held in place, allowing for easy separation of the gas or liquid reagents from the solid catalyst [22].

In contrast to a telescoped system, a batch cascade is where multiple reactions occur in a single reactor flask without intermediate workup. Batch cascades are a promising way to reduce the required number of unit operations in a synthesis and increase atom economy [36,37]. However, batch cascades require multi-functional catalysts or else using multiple catalysts in the same flask that do not negatively interfere with each other. Additionally, all reactions must occur at the same temperature and pressure. These requirements result in a constrained design space and it is anticipated that switching from batch cascade to telescoped flow, where the reactions are separated into different reactors, could alleviate these requirements and allow for process intensification. The objective of this work is to convert a recently published batch cascade process to a telescoped flow process to demonstrate the widened design space offered by telescoped systems, as well as highlighting the difficulties in converting a multistep synthesis from batch to flow.

The reaction systems studied in this work are the multistep synthesis of benzylacetone (**4**) from benzyl alcohol (**1**) and of 4-(4-methoxyphenyl)butan-2-one (**4**) from 4-methoxybenzyl alcohol (**1**), via oxidation, aldol condensation and reduction, as shown in Fig. 1. Note that the oxidation step produces a number of side products, as multiple

reactions occur in parallel including dehydrogenation, disproportionation and hydrogenolysis [38]. Two feed molecules were studied to examine the flexibility of the flow system to different substituted groups, as in some cases the batch cascade showed dramatically different yields for different substituted feed molecules [39]. These reaction systems were chosen as the products have high commercial value as food additives, insect attractants and fragrances [39,40] and because the recently developed batch cascade was more selective and produced less waste than current commercial production methods using Friedel-Crafts alkylations [40,41]. The catalysts used in the batch study were Au-Pd nanoparticles supported on MgO or TiO₂, and the optimum catalyst was found to be AuPd/MgO [39]. However, it was not possible to use MgO supported catalysts in flow, as the MgO support did not retain its mechanical integrity; particles broke into smaller ones leading to blockages during prolonged use. The instability of MgO particles is attributed to the hydroxylation of MgO to Mg(OH)₂ in the presence of water, which has been previously reported for this system [39,42]. Therefore only TiO₂ supported catalysts were available for use in the telescoped system. All three of these reaction steps have been reported in the literature with a variety of different catalysts and reactor types, however, this work is the first to perform the telescoped synthesis in flow. Benzyl alcohol oxidation with molecular oxygen has been studied extensively [43–51] in both solvent and solvent free conditions, and the catalyst used in this work, AuPd/TiO₂ is one of the most active, as it can achieve TOF greater than 10,000 h⁻¹ [50], reasonable selectivity [46] and its deactivation behaviour has been optimised [47]. Aldol condensation reactions are known to benefit from bifunctional catalysts which possess both acid and basic sites [52] and they have been studied with a wide range of catalysts including metal oxides (MgO, ZrO₂ and TiO₂) [53–55], double layered hydroxides [56] and amine-functionalised SBA-15, ZrO₂ and TiO₂ [52]. In this work, anatase TiO₂ was chosen because it was desired to use the same catalysts as in the batch study [39]. The reduction of benzalacetone has been successfully demonstrated using Pd nanoparticles in packed beds [57] and in monolith reactors [58] and in this work both Pd/TiO₂ and Pt/TiO₂ were tested in packed bed reactors.

2. Materials and methods

2.1. Catalyst preparation

The 1 wt% 65:35 (weight ratio) Au:Pd/TiO₂ catalyst was prepared by a modified impregnation method, where a round bottom flask was charged with H₂AuCl₄ (0.53 mL, 12.25 mgAu/mL), PdCl₂ dissolved in 0.58 M HCl (0.97 mL, 6 mgPd/mL) and water (13.5 mL) following a method described in previously published work [47]. The monometallic 1 wt% Pd/TiO₂ and Pt/TiO₂ catalysts were prepared by impregnation, where the metal salt PdCl₂ or PtCl₂ was dissolved in a small amount of

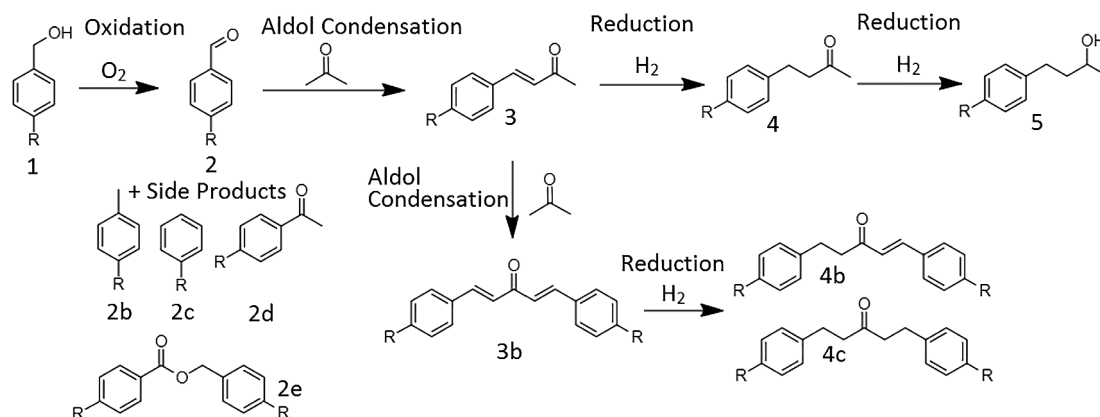


Fig. 1. Reaction chemistry for the multistep synthesis of (**4**), benzylacetone (R = H) and 4-(4-methoxyphenyl)butan-2-one (R = OCH₃).

water, to which TiO₂ was added. The slurry was stirred and heated until a paste was formed, then dried (110 °C, 16 h) and later calcined at 400 °C for 3 h. For all the supported nanoparticle catalysts used, the TiO₂ support was P25 TiO₂ (Evonik). TiO₂ was used as a coupling catalyst and initially a 21 nm particle size nanopowder (Sigma Aldrich, 99.5% pure, 75% anatase and 25% rutile) was used. However, after studying the coupling reaction in isolation it was found that pure anatase TiO₂ was more active and subsequently for all telescoped experiments a 31 nm nanopowder anatase TiO₂ was used (Alfa Aesar). All of the catalysts used in this study were pelletised with 4000 N force using a pellet press, then ground and sieved to give the appropriate particle size range, typically 63–75 μm or 90–120 μm. The proportion of catalyst attaining the desired sieve fraction was 10–20%. BET studies showed only a small reduction in surface area, from 58.7 m²/g to 53.65 m²/g after pelletisation.

2.2. Reactor design & experimental set up

The reactions were carried out in both silicon-glass microreactors and in tube capillary reactors. The silicon-glass microreactors consisted of serpentine channels of dimensions 600 μm width, 300 μm height and 190 mm length with rectangular posts at the outlet to retain the solid catalyst. These reactors have been used in earlier work and their fabrication using photolithography and DRIE is described elsewhere [49]. The tube capillary reactors consisted of PTFE tubing with 1.587 mm O.D. and 1 mm I.D. (VICI Jour). The catalyst was retained in the tubing by use of a nickel mesh (Tecan, UK) of 25 μm thickness and 25 μm diameter holes which was held in place with compressive force between a PEEK union (Upchurch) and a PEEK ferrule (Upchurch). The tube reactor was used when the catalyst mass required surpassed the maximum catalyst loading of the silicon-glass microreactors (approximately 40 mg of TiO₂). The silicon-glass reactor was heated using heating cartridges in a chuck enclosed in ceramic packaging for insulation, while the tube reactor was heated in a stirred oil bath. In both cases the catalysts were loaded into the reactors by applying vacuum to the reactor outlet and introducing a known mass of catalyst through the reactor inlet. The reactors were weighed before and after loading to measure the mass of catalyst.

A number of experiments were conducted including studying the oxidation, coupling and reduction reactions independently and also in series. Additionally, in many cases when studying reactions in isolation small amounts of likely impurities (side products, unreacted reagents from upstream reactions) were added to study reaction inhibition. The experimental set-up varied depending on the reaction(s) being studied, but in all cases the same equipment was used. Liquid feeds (alcohol in acetone solution) were introduced using stainless steel 8 mL syringes (Harvard Apparatus) and syringe pumps (Harvard Apparatus, Ph.D. Ultra). The gases were fed using mass flow controllers (Brooks 5850TR) and the pressure at the reactor outlet was controlled using a back pressure regulator (Swagelok KBP series, 250 PSIG). The liquid product was collected in a custom made PEEK collection vessel, which separated the liquid from the gas via gravity. A schematic of the experimental set-up for gas-liquid-solid reactions, such as the oxidation and reduction reactions, is shown in Fig. 2. For liquid-solid experiments (coupling reaction) the gas inlet on the microreactor chip was closed and the system was pressurised with nitrogen gas flowing directly into the PEEK collection vessel.

The experimental set-up for the telescoped flow system is shown in Fig. 3, where the reactors were connected in series with a tube-in-tube membrane separator immediately after the oxidation reactor to remove the oxygen gas. The membrane separator consisted of a 65 cm long Teflon AF-2400 tubular membrane (Biogeneral, U.S.) of I.D. 0.8 mm and thickness 0.1 mm within a 3.175 mm O.D., 2.4 mm I.D. PTFE tube (VICI Jour). The tube-in-tube membrane device operated with the gas-liquid flow in the inner tube at 6 bar pressure while the outer tube was connected to a vacuum pump (KNF labs) providing –500 mbar

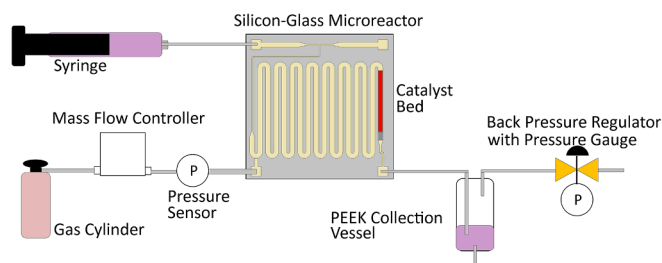


Fig. 2. Experimental set-up for gas-liquid-solid reactions in a silicon-glass microreactor.

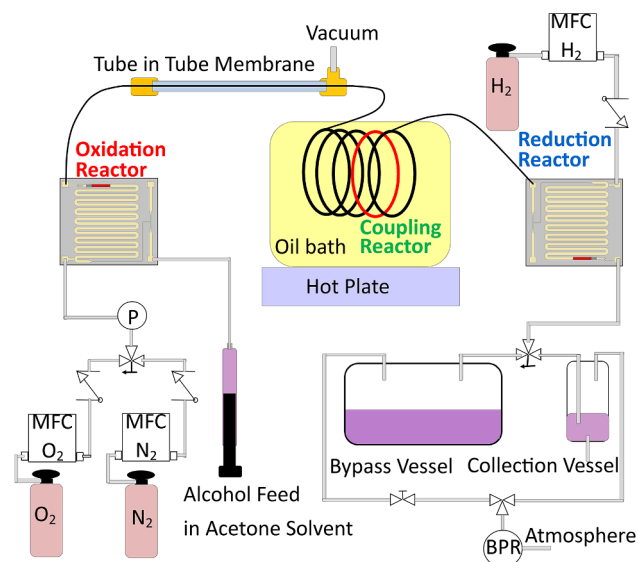


Fig. 3. Experimental set-up for the multistep synthesis of benzylacetone and 4-(4-methoxyphenyl)butan-2-one. The red sections in the reactors represent the catalyst packed bed, MFC (mass flow controller), BPR (back pressure regulator) and P (pressure sensor).

vacuum. In the literature, such Teflon AF-2400 membranes operated satisfactorily at even higher pressure differences of 13 bar [59] or at elevated temperatures of 120 °C [45].

2.3. Product analysis

The liquid product was analysed off-line using gas chromatography (Agilent, 7820A) with a FID detector and an Agilent DB-624 capillary column. Mesitylene was used as an internal standard to allow for volume change corrections associated with the generation of water and the loss of acetone through evaporation upon sample collection and depressurisation. A carbon balance where the concentration of the reactant in the feed was compared to the concentration of the reaction products in the outlet stream is shown in Eq. (1), where C represents concentration (M) and p_i and f represent the stoichiometric coefficients of the i -th product species and the alcohol feed ($f = 1$). For the benzylacetone system the carbon balance was found to close within 95% when studying reactions in isolation, and to within 70–90% when studying the entire multistep system. All chemical species; benzyl alcohol (1), benzaldehyde (2), toluene (2b), benzene (2c), benzoic acid (2d), benzyl benzoate (2e), benzalacetone (3), dibenzalacetone (3b), benzylacetone (4), 4-phenylbutan-2-ol (5), 4-methoxybenzyl alcohol (1), 4-methoxybenzaldehyde (2), 4-methylanisole (2b), anisole (2c), 4-(4-methoxyphenyl) butan-2-one (4), 4-(4-methoxyphenyl)butan-2-ol (5), acetone and mesitylene were from Sigma Aldrich.

$$\text{Carbon Balance} = \frac{C_{\text{Reactant In}} - \left(C_{\text{Reactant Out}} + \sum \frac{f}{P_i} * C_{i\text{Product Out}} \right)}{C_{\text{Reactant In}}} \quad (1)$$

Reactant feed conversion X , was calculated using Eq. (2) and the selectivity S_i , using Eq. (3). When studying reactions in isolation the average reaction rate, r_{av} (mol/s/g catalyst) was calculated according to Eq. (4), where m is the catalyst mass (g) and v is the inlet liquid flowrate (L/s). The reaction rate varies along the length of the packed bed, however this average reaction rate is still a useful parameter for comparison purposes. The yield of the reaction to each species i , Y_i represents the fraction of the reagent that forms species i , and it was calculated according to Eq. (5) which takes into account the reaction stoichiometry. The catalyst contact time in flow was calculated by dividing the catalyst mass by the mass flowrate of alcohol, as shown in Eq. (6). In the batch system the catalyst contact time was calculated by dividing the product of reaction time t and catalyst mass by the mass of alcohol in the reactor, which is given by the product of the reactor volume V , feed concentration and molecular weight of the feed alcohol MW_{Reactant} as shown in Eq. (7). When studying the reactions in isolation, the coupling and reduction catalysts were observed to undergo considerable deactivation, with up to 50% loss in activity in 8 h of operation. For this reason fresh catalyst was used every day and a deactivation correction procedure assuming linear deactivation was applied as discussed in the [Supplementary Information](#). Error bars represent 1 standard deviation calculated from triplicate sampling.

$$X = \frac{C_{\text{Reactant In}} - C_{\text{Reactant Out}}}{C_{\text{Reactant In}}} \quad (2)$$

$$S_i = \frac{\frac{f}{P_i} * C_{\text{Desired Product}}}{C_{\text{Reactant In}} - C_{\text{Reactant Out}}} \quad (3)$$

$$r_{av} = \frac{(C_{\text{Reactant In}} - C_{\text{Reactant Out}})v}{m} \quad (4)$$

$$Y_i = \frac{C_{i\text{Out}} * \frac{f}{P_i}}{C_{\text{Reactant In}}} \quad (5)$$

$$\text{Flow Catalyst Contact Time} = \frac{m}{v * MW_{\text{Reactant}} * C_{\text{Reactant}}} \quad (6)$$

$$\text{Batch Catalyst Contact Time} = \frac{t * m}{V * MW_{\text{Reactant}} * C_{\text{Reactant}}} \quad (7)$$

3. Results & discussion

3.1. Batch cascade vs telescoped flow

The telescoped flow synthesis of both benzylacetone and 4-(4-methoxyphenyl)butan-2-one were successfully performed using the experimental set-up shown in [Fig. 3](#). For both feed molecules the same catalysts were used (1 wt% AuPd/TiO₂, anatase TiO₂ and 1 wt% Pt/TiO₂) and the standard experimental conditions were 115 °C, 130 °C and 120 °C for the oxidation, coupling and reduction reactions, 2 NmL/min oxygen gas flowrate and 1.5 NmL/min hydrogen flowrate with the system back pressure regulator set to 5 barg. Variable feed concentrations, liquid flowrates and catalyst masses were used for both systems. The operating conditions were chosen based on information obtained studying the reactions in isolation by performing parametric studies (varying liquid and gas flowrates, temperature, pressure and particle sizes), which is discussed in the [Supplementary Information](#).

Maximum yields of 56% for benzylacetone were obtained in telescoped flow when using the most dilute feed concentrations studied (0.72 M). This is a major increase on the 8% yield obtained in batch as shown in [Fig. 4](#) [39], however the low batch yield may be partially due to the fact that the batch system was optimised for the 4-methoxybenzyl

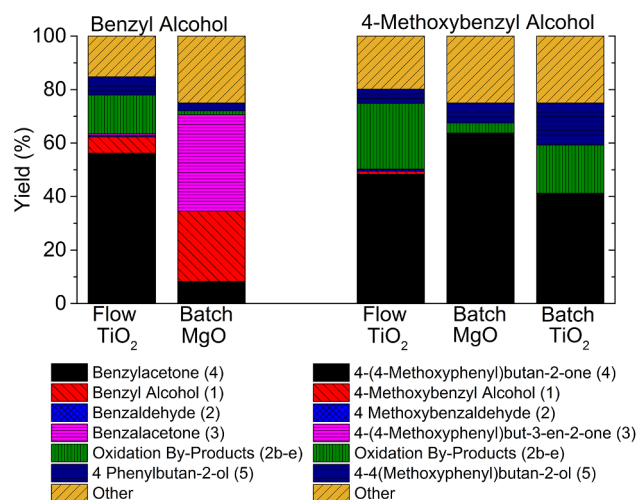


Fig. 4. Yields of the benzylacetone and 4-(4-methoxyphenyl)butan-2-one systems for both the one-pot and flow experiments. In flow, only TiO₂ supported catalysts were used but in batch TiO₂ or MgO were used. The flow data is from the most dilute experiments conducted (0.72 M benzyl alcohol, 0.75 M 4-methoxybenzyl alcohol) which produced the highest yield of the desired product. Both flow systems were run at the standard temperatures, pressure and gas flows. The benzyl alcohol flow system had a liquid flowrate of 40 μL/min and 10.4 mg, 223 mg and 12.0 mg of catalysts for the oxidation, coupling and reduction reactions respectively. The methoxybenzyl alcohol flow system had a flowrate of 10 μL/min and 10.1 mg, 152 mg and 9.5 mg of catalysts for the oxidation, coupling and reduction reactions respectively. Data for the one-pot experiments was taken from [39]. The batch experiments used 500 mg of 1 wt% AuPd/supported catalysts at 5 barg for 22 h and with feed concentration approximately 0.9 M, the reaction temperature was 75 °C for the TiO₂ support and 125 °C for the MgO support experiments.

alcohol feed and not the benzyl alcohol feed. The yield from the batch synthesis was calculated by multiplying the reported conversion by the reported selectivity and multiplying again by a factor for the unidentified species, as the reported selectivity was calculated as the fraction of desired product over the sum of all identified species (only 70–80% of species were identified) [39]. The dramatic increase in yield is attributed to the greater flexibility of the telescoped flow system being able to perform each reaction in a separate reactor, allowing the choice of different catalysts and operating condition for each reaction. It is also expected that the multistep flow system has greater potential for optimisation. In this work the choice of catalyst was limited to those previously used in batch to focus on the study of the reactor system and widened design space instead of catalyst performance. However, if more suitable aldol condensation catalysts were used, such as metal oxides (ZrO₂) [53–55], double layered hydroxides [56] and amine-functionalised SBA-15, ZrO₂ and TiO₂ [52], then it is expected that even better performance could be achieved.

As shown in [Fig. 4](#), the telescoped flow system showed a higher yield of the 4-(4-methoxyphenyl)butan-2-one than the one-pot synthesis when both systems used TiO₂ supported catalysts (48% compared to 41%). However, when the batch system used the MgO catalyst, the yield exceeded that achieved in flow (48% compared to 63%). This was largely because the AuPd/TiO₂ catalyst which was used in flow, was not able to achieve the high selectivity in the oxidation reaction that the AuPd/MgO catalyst was able to achieve in batch. Unfortunately, it was not possible to use the MgO support in micropacked bed reactors, as the support particles broke into smaller particles and clogged the reactors. This demonstrates a drawback of current telescoped flow systems, in that the catalyst must be compatible with packed beds as current slurry reactors which retain the slurry in the reactor (via filtration at the reactor exit) are not reliable enough to integrate with a telescoped system. The majority of reliable slurry reactors today instead have the slurry passing out of the reactor outlet [28–35].

The main advantage of the multistep flow system was not just in yield improvement but in smaller catalyst requirements and increased productivity. Primarily, the multistep flow system allowed for the replacement of significant amounts of the expensive nanoparticle supported catalysts with the cheaper TiO₂ catalyst. To process a similar amount (0.01 mol) of either feed alcohol, the batch system used 500 mg of AuPd supported catalyst, while the flow system used only 20 mg nanoparticle supported catalysts (approximately 10 mg of AuPd/TiO₂ and 10 mg of Pt/TiO₂) and 150–250 mg of the cheap anatase TiO₂. Additionally, although the catalyst contact time per gram of alcohol varied in the flow experiments due to the range of inlet liquid flowrates, feed concentrations and catalyst masses used, the experiments still suggest that the catalyst was being used more efficiently in flow than in batch. For the benzylacetone experiment shown in Fig. 4, which produced the maximum yield, the catalyst contact times were only 55 h mg_{catalyst}/g_{alcohol} and 65 h mg_{catalyst}/g_{alcohol} for the oxidation and reduction reactions and 1190 h mg_{catalyst}/g_{alcohol} for the coupling reaction. In comparison, in the one-pot system the catalyst contact time was calculated by dividing the product of reaction time (22 h) and catalyst mass (500 mg) by the mass of alcohol (1.3 g), and for the benzylacetone one-pot system this was 8460 h mg_{catalyst}/g_{alcohol}. Thus, the total amount of catalysts utilised in the benzyl alcohol multistep flow system was approximately 6.5 times lower than in the one-pot system. For the 4-methoxybenzyl alcohol system the same comparisons are harder to make, as the batch reaction reached completion before the end of the 22 h.

3.2. Catalyst inhibition

It was found that the yield of the telescoped flow system decreased with increasing feed concentration, as shown in Figs. 5 and 6. While this was partly due to the decreasing catalyst contact time, it was discovered that the coupling reaction in the multistep system suffered from extreme water inhibition due to the generation of water in both the oxidation and coupling reactions. This resulted in the requirement

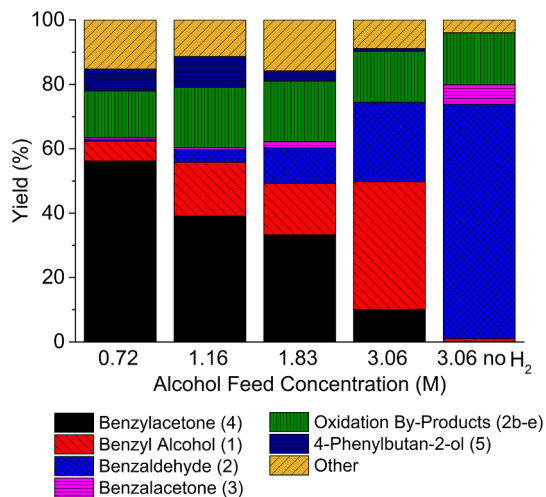


Fig. 5. Yield of reaction products from the multistep flow synthesis of benzylacetone in flow at four different inlet concentrations of benzyl alcohol, and from an experiment where no hydrogen gas was used (to prevent the reduction reaction). The standard experimental conditions of temperatures, pressure and gas flows were used. The mass of oxidation and reduction catalysts were approximately 10 mg for all experiments. The inlet liquid flowrate and coupling catalyst mass varied for different experiments to keep the coupling catalyst contact time to a similar value between experiments; the coupling catalyst mass was approximately 250 mg for the 0.72 M and 1.16 M experiments and 150 mg for the 1.83 M and 3.06 M experiments, while the inlet liquid flowrate was 40 $\mu\text{L}/\text{min}$, 40 $\mu\text{L}/\text{min}$, 10 $\mu\text{L}/\text{min}$ and 20 $\mu\text{L}/\text{min}$ for the 0.72 M, 1.16 M, 1.83 M and 3.06 M experiments respectively.

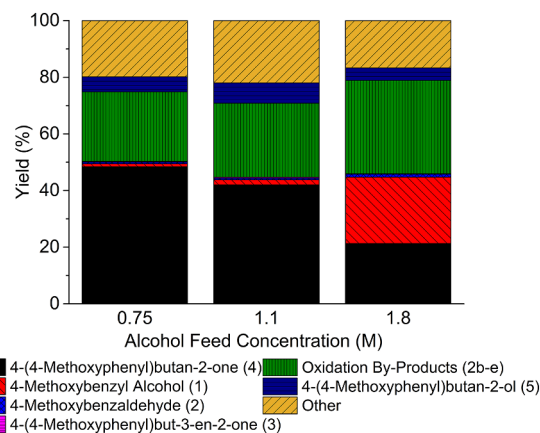


Fig. 6. Yield of reaction products from the multistep flow synthesis of 4-(4-methoxyphenyl)butan-2-one in flow at three different inlet concentrations of 4-methoxybenzyl alcohol. The liquid flowrate was 10 $\mu\text{L}/\text{min}$ and the standard experimental conditions for temperatures, pressure and gas flowrates were used with 10 mg, 150 mg and 10 mg of catalysts for the oxidation, coupling and reduction reactions respectively.

of using dilute feed concentrations of less than 1.3 M as well as using excess TiO₂ to compensate for reduced activity. The water inhibition can be seen in Fig. 5, where the amount of unreacted alcohol (1) and unreacted aldehyde (2) was significantly higher for the 3.06 M feed than the other lower concentration experiments. The result of the 3.06 M feed experiment shown in Fig. 5 suggests that both the oxidation and coupling reactions could be inhibited by high feed concentrations, as there were large amounts of unreacted benzyl alcohol (1) as well as benzaldehyde (2). However, it was later demonstrated that only the coupling reaction was inhibited by water and not the oxidation reaction, which proceeded with near 100% conversion in all cases. The benzyl alcohol (1) in the outlet stream was actually produced from the reduction of unreacted benzaldehyde (2) in the reduction reactor. This was confirmed in the 3.06 M experiment by replacing the hydrogen gas with nitrogen in the reduction reactor; the amount of unreacted benzyl alcohol then dropped to almost zero and the yield of unreacted benzaldehyde rose dramatically to 70%. Studies of the coupling reaction in isolation showed that water concentration of just 2.75 wt% resulted in a 50% drop in activity, as shown in the Supplementary Information. Assuming complete conversion of all benzyl alcohol feed, a feed concentration of only 1.3 M would produce the 2.75 wt% water necessary for water inhibition. This suggests that the 1.83 M experiment in Fig. 5 is also suffering from water inhibition, but that there is a sufficient excess of TiO₂ catalyst to partially compensate for this. The reduction reaction was also found to be inhibited by water. However, a higher concentration of water was required to inhibit the reduction reaction than the coupling reaction; hence this did not impose any extra design constraints on the multistep flow system. The same water inhibition was observed in the synthesis of 4-(4-Methoxyphenyl)butan-2-one as shown in Fig. 6.

The coupling reaction was inhibited by even very low concentrations of benzoic acid (2d); just 0.03 M benzoic acid in the coupling reactor feed stream led to a drop in the reaction rate of 30%. Unfortunately, trace amounts of benzoic acid are unavoidable in the oxidation reaction and even after attempting to tune the reaction conditions to minimise its formation, the concentration of benzoic acid was approximately 0.03 M resulting in some inhibition. Inhibition studies conducted for the reduction reaction in isolation also showed that the reduction reaction was inhibited by various organic species, including benzaldehyde (2) and dibenzylacetone (3b) as shown in the Supplementary Information. However, this was not found to be significant in the telescoped flow system, as the concentration of the inhibiting by-products did not reach the high values that were added to

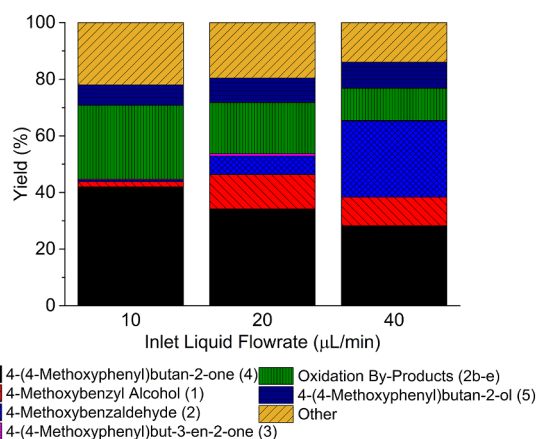


Fig. 7. Yield for the 4-(4-methoxyphenyl)butan-2-one system at three different inlet liquid flowrates using a 1.1 M feed of 4-methoxybenzyl alcohol. The standard experimental conditions for temperatures, pressure and gas flowrates were used with 10 mg, 149 mg and 11 mg of catalysts for the oxidation, coupling and reduction reactions respectively.

the feed solution in the isolated inhibition studies. Furthermore, the rate of the reduction reaction was sufficiently high that a certain level of inhibition was tolerable and could be offset by an increase in the catalyst mass, especially in comparison to the much slower coupling reaction.

3.3. Effect of catalyst contact time

The effect of catalyst contact time was investigated for both the benzylacetone and the 4-(4-methoxyphenyl)butan-2-one system by changing the inlet liquid feed flowrate while keeping all other conditions constant. The results in Fig. 7 for the 4-(4-methoxyphenyl)butan-2-one system, show the expected trend that at lower catalyst contact times the conversion of both the oxidation and the coupling reaction decreased. However, when the oxidation reaction was carried out at similar conditions or even with a lower catalyst contact time than that used in the telescoped system (9.4 mg of 1 wt% AuPd/TiO₂ at 115 °C, 2 NmL/min O₂ flowrate, 20 μL/min liquid flowrate of 0.96 M 4-methoxybenzyl alcohol feed at 6 bar back pressure) greater than 95% conversion was achieved. Therefore it is suspected that the unreacted alcohol (1) in the outlet is not due to lower performance in the oxidation reactor but due to unreacted aldehyde (2) being converted back to alcohol in the reduction reactor. The same trend was observed for the benzylacetone system, as shown in the [Supplementary Information](#).

3.4. Oxygen separation

The removal of oxygen gas was found to be critical in the multistep flow synthesis for a number of reasons including safety and optimising the coupling and reduction reactions. While microreactors are known for their increased safety [60,61], oxygen gas removal was performed to prevent oxygen mixing with hydrogen gas downstream and creating an explosive atmosphere in the bypass vessel, which had a sufficiently large volume (200 mL) to present a hazard under the high operation pressure. It was also discovered that the rate of the coupling reaction dropped significantly if either the liquid feed was allowed to vaporise or if any gas was flowing with the liquid; this is shown in the [Supplementary Information](#). This prevented the integration of the coupling reaction with either the oxidation or reduction reactions and it required oxygen gas removal immediately after the oxidation reaction. It is possible that the decrease in coupling reaction rate in the presence of gas was due to loss of acetone in the liquid phase by evaporation, leading to a lower concentration available for reaction and increased

difficulty in removing the resultant products from the catalyst surface. The removal of oxygen gas was achieved using a tube-in-tube membrane, as complete removal of oxygen could be reliably achieved even under conditions where pressure fluctuated significantly, such as during sample taking or when changing the flowrates. In addition to oxygen, acetone also permeated through the membrane and was lost from the reaction mixture in low quantities (approximately 7% of the initial acetone was lost to evaporation, when the initial concentration of acetone was typically 9 M or 70% by mass of the feed solution), but this loss was considered acceptable.

3.5. Coupling catalyst issues and effect on telescoped reactor design

The coupling reaction was found to be a bottleneck in this system, as its reaction rate without any impurities in the feed was only 1.5×10^{-5} mol/g/s, approximately an order of magnitude lower than that of the oxidation or reduction reactions, and then its reaction rate was further reduced due to catalyst inhibition as mentioned previously. The low reaction rate led to the use of more than 150 mg of anatase TiO₂, which exceeded the 40 mg maximum capacity of the silicon-glass microreactors, requiring the use of a packed tube reactor. This larger packed bed caused a pressure drop of about 1.5 bar and due to its large catalyst mass it clogged on more than one occasion. The maximum inlet liquid flowrate was limited at 40 μL/min, as higher flowrates required even longer catalyst beds, greater pressure drops and increased the likelihood of clogging the reactor. Therefore this catalyst restricted the maximum liquid flowrate possible and hence limited the productivity of this system. Furthermore, heating the packed tube in an oil bath required long connection tubing that increased the system residence time.

The study of the coupling reaction, included in the [Supplementary Information](#), suggests that this catalyst may not be ideal for the multistep flow system, and other catalysts may provide improved performance. The key findings regarding the coupling reaction were that at temperatures > 120 °C, which are the best operating conditions for the multistep system, the reaction shows significant external mass transfer resistances and is inhibited by the product. The external mass transfer resistances are demonstrated in Fig. 8 at high temperatures of 140 °C, where the rate of reaction increased with increasing liquid flowrate for a constant catalyst contact time. At lower temperature of 100 °C external mass transfer resistances are not observed, indicating that the

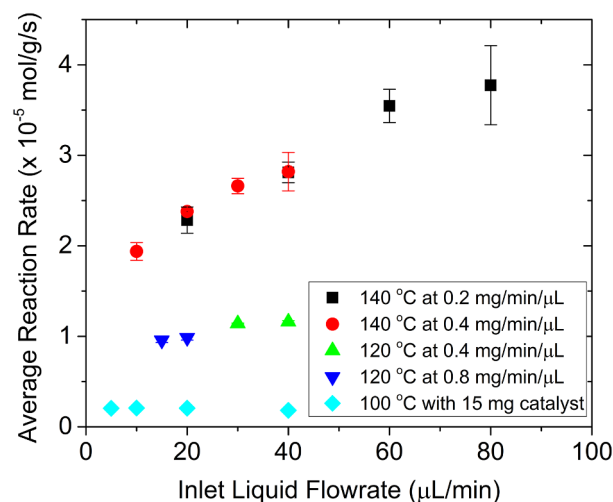


Fig. 8. Average reaction rate (corrected for deactivation) against inlet liquid flowrate for the coupling reaction of benzaldehyde with acetone. Experimental conditions were 6 barg, 2.2 M benzaldehyde in acetone, 63–75 μm TiO₂ catalyst. Catalyst amounts were chosen to give the desired catalyst contact times (mg/min/μL), except of the 100 °C experiment where 15 mg of catalyst was used for all experiments.

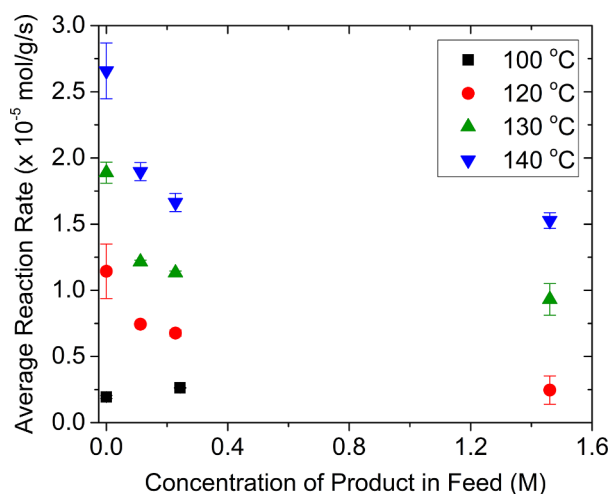


Fig. 9. Average reaction rate (corrected for deactivation) against concentration of the product benzalacetone in the feed stream for the coupling reaction of benzaldehyde with acetone. Experimental conditions were 6 barg, 10 $\mu\text{L}/\text{min}$ inlet liquid feed rate of approximately 2.8 M benzaldehyde in acetone, 8 mg of 63–75 μm TiO_2 catalyst. In addition to benzalacetone (**3**), the side product dibenzalacetone (**3b**) was added to the feed at approximately 20% of the benzalacetone concentration.

reaction swaps from kinetic control to mass transfer control between these two temperatures. Note that all the data points corresponded to a conversion of less than 40%, explaining why the catalyst contact time had a minimal effect on reaction rate. Product inhibition is shown in Fig. 9 where the rate of reaction decreases as increasing concentrations of the product benzalacetone (**3**) and side product dibenzalacetone (**3b**) are added to the feed solution. This information suggested that this anatase TiO_2 catalyst was not very suitable for a multistep flow system where 100% conversion is required. This conclusion was reached for two reasons. Firstly, 100% conversion would lead to product inhibition except in the case of very dilute feed. This catalyst would be much more efficient operating at lower conversions. Secondly, this catalyst operates best at high liquid flowrates to reduce mass transfer resistances, but if 100% conversion is required it is not possible to use high flowrates as a large catalyst bed will be needed and the high flowrates would cause unreasonable pressure drop. However, despite the challenges this catalyst created, it was still possible to find flow operating conditions that produced a high yield of the final product. This demonstrates that in a situation when one must use a given catalyst it is still possible to convert from batch to flow, but also that further optimisation can be achieved by improving the catalyst.

3.6. Catalyst deactivation

Deactivation was found to be a serious problem in the batch cascade study, where reusing catalyst from one batch to the next led to a fall in conversion from 100% to 46% after a single use in hydrogen atmosphere and from 96% to 0% in nitrogen atmosphere [39]. Deactivation has also been observed in flow for the oxidation of benzyl alcohol, where it was shown to be related to the catalyst formulation and preparation method [47]. Similarly, in this multistep flow system deactivation was also found to be a significant problem. Deactivation of up to 50% in 8 h of operation was observed when studying the coupling and reduction reactions in isolation, where a colour change of the catalyst was observed, forming a front that travelled down the length of the packed bed (shown in the Supplementary Information). This colour change provides further evidence to the hypothesis originally suggested in the batch study that deactivation is linked to adsorption of carbon species on the catalyst surface [39]. The problem of using deactivating catalysts in telescoped systems could be partially overcome by using an

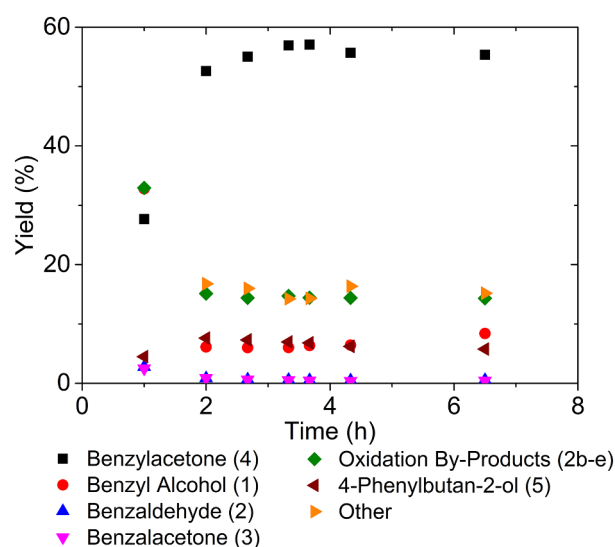


Fig. 10. Deactivation study for the benzylacetone telescoped system, showing yield of various products against operation time. The standard experimental conditions of temperatures, pressure and gas flowrates were used with 10.4 mg, 223 mg and 12.1 mg of oxidation, coupling and reduction catalysts respectively and an inlet liquid flowrate of 40 $\mu\text{L}/\text{min}$ of 0.7 M benzyl alcohol in acetone.

excess of catalyst. This was demonstrated for the benzylacetone telescoped system, as the yield of benzylacetone remained stable after 6.5 h of continuous operation, as shown in Fig. 10. While the duration of this flow experiment (6.5 h) is far shorter than the batch (22 h), the amount of alcohol processed (0.01 mol in flow and 0.009 mol in batch) is comparable, hence showing that the effect of deactivation in flow was reduced. Despite the relative stability of the system over the 6.5 h experiment, catalysts with higher stability would be needed for industrial application.

4. Conclusions

The multistep synthesis of benzylacetone and 4-(4-methoxyphenyl)butan-2-one using AuPd, Pd and Pt supported catalysts was successfully converted from batch cascade to a telescoped flow system demonstrating both the advantages and challenges of flow systems. The most critical advantage of the telescoped flow system compared to the batch cascade was the ability to separate the three reactions, oxidation, coupling and reduction, hence allowing more freedom to choose different catalysts and operating conditions without the necessity of finding a compromise among reactions. In this case this freedom enabled process intensification, reducing catalyst contact requirements by a factor of 6.5 for the benzylacetone system and allowing the replacement of significant amounts of expensive nanoparticle supported catalysts with cheaper anatase TiO_2 catalyst. Additionally, the flow system attained higher yields of 4-(4-methoxyphenyl)butan-2-one than the batch system when both systems used TiO_2 supported catalysts (48% compared to 41%). However, the drawback of the telescoped flow system was that it was not possible to use the MgO supported catalyst that was found to be better for this reaction in the batch cascade, due to the MgO not having suitable mechanical properties to be used in a micropacked bed. This resulted in the telescoped flow system not being able to achieve the highest yield to 4-(4-methoxyphenyl)butan-2-one of 63%, which was achieved in batch with the MgO supported catalyst. Despite this drawback, the telescoped flow system with TiO_2 supported catalysts was able to outperform the batch flow system with the preferred MgO supported catalysts for the synthesis of benzylacetone (56% compared to 8%). While in this work the selection of catalysts for the telescoped flow system was restricted to those used in batch to focus on the effect of reactor configuration (batch vs flow), it is expected that the

performance of the telescoped flow system could be improved if the choice of catalysts is extended beyond the nanoparticle supported catalysts previously used in the batch system. This would be taking full advantage of the telescoped flow system's extended design space and may overcome some of the challenges encountered in this work, including water and product inhibition.

Acknowledgements

The authors thank EPSRC, UK for funding (Grants EP/J017868/1 and EP/J017833/1) and also Dr Anand Pallipurath for his assistance in experiments.

Appendix A. Supplementary data

Supplementary data to this article can be found online at <https://doi.org/10.1016/j.cej.2018.09.137>.

References

- [1] A. Adamo, R.L. Beingessner, M. Behnam, J. Chen, T.F. Jamison, K.F. Jensen, J.-C.M. Monbaliu, A.S. Myerson, E.M. Revalor, D.R. Snead, T. Stelzer, N. Weeranoppanant, S.Y. Wong, P. Zhang, On-demand continuous-flow production of pharmaceuticals in a compact, reconfigurable system, *Science* 352 (2016) 61–67.
- [2] F. Lévesque, P.H. Seeberger, Continuous-flow synthesis of the anti-malaria drug artemisinin, *Angew. Chem. Int. Ed.* 51 (2012) 1706–1709.
- [3] R. Örkényi, J. Éles, F. Faigl, P. Vincze, A. Prechl, Z. Szakács, J. Kóti, I. Greiner, Continuous synthesis and purification by coupling a multistep flow reaction with centrifugal partition chromatography, *Angew. Chem. Int. Ed.* 56 (2017) 8742–8745.
- [4] M. Baumann, I.R. Baxendale, The synthesis of Active Pharmaceutical Ingredients (APIs) using continuous flow chemistry, *Beilstein J. Org. Chem.* 11 (2015) 1194.
- [5] A.R. Bogdan, S.L. Poe, D.C. Kubis, S.J. Broadwater, D.T. McQuade, The continuous-flow synthesis of ibuprofen, *Angew. Chem. Int. Ed.* 48 (2009) 8547–8550.
- [6] B. Gutmann, D. Cantillo, C.O. Kappe, Continuous-flow technology—a tool for the safe manufacturing of active pharmaceutical ingredients, *Angew. Chem. Int. Ed.* 54 (2015) 6688–6728.
- [7] T. Tsubogo, H. Oyamada, S. Kobayashi, Multistep continuous flow synthesis of (R)- and (S)-rolipram using heterogeneous catalysts, *Nature* 520 (2015) 329–332.
- [8] J.L. Howard, C. Schotten, D.L. Browne, Continuous flow synthesis of antimalarials: opportunities for distributed autonomous chemical manufacturing, *React. Chem. Eng.* 2 (2017) 281–287.
- [9] S. Borukhova, T. Noël, V. Hessel, Continuous-flow multistep synthesis of cinnarizine, cyclizine, and a buclizine derivative from bulk alcohols, *ChemSusChem* 9 (2016) 67–74.
- [10] J. Guan-Young, K.S. Ajay, S. Siddharth, G. Ki Won, M. Ram Awatar, K. Dong-Pyo, One-flow syntheses of diverse heterocyclic furan chemicals directly from fructose via tandem transformation platform, *NPG Asia Mater.* 7 (2015) e173.
- [11] J.Q. Bond, D.M. Alonso, D. Wang, R.M. West, J.A. Dumesic, Integrated catalytic conversion of γ -valerolactone to liquid alkenes for transportation fuels, *Science* 327 (2010) 1110–1114.
- [12] E.L. Kunkes, D.A. Simonetti, R.M. West, J.C. Serrano-Ruiz, C.A. Gärtner, J.A. Dumesic, Catalytic conversion of biomass to monofunctional hydrocarbons and targeted liquid-fuel classes, *Science* 322 (2008) 417.
- [13] J. Britton, C.L. Raston, Multi-step continuous-flow synthesis, *Chem. Soc. Rev.* 46 (2017) 1250–1271.
- [14] I.R. Baxendale, J. Deeley, C.M. Griffiths-Jones, S.V. Ley, S. Saaby, G.K. Tranmer, A flow process for the multi-step synthesis of the alkaloid natural product oxomartidine: a new paradigm for molecular assembly, *Chem. Commun.* (2006) 2566–2568.
- [15] A.R. Bogdan, M. Charaschanya, A.W. Dombrowski, Y. Wang, S.W. Djuric, High-temperature Boc deprotection in flow and its application in multistep reaction sequences, *Org. Lett.* 18 (2016) 1732–1735.
- [16] D. Cantillo, B. Wolf, R. Goetz, C.O. Kappe, Continuous flow synthesis of a key 1,4-benzoxazinone intermediate via a nitration/hydrogenation/cyclization sequence, *Org. Process Res. Dev.* 21 (2017) 125–132.
- [17] X. Liu, K.F. Jensen, Multistep synthesis of amides from alcohols and amines in continuous flow microreactor systems using oxygen and urea hydrogen peroxide as oxidants, *Green Chem.* 15 (2013) 1538–1541.
- [18] T. Noël, S. Kuhn, A.J. Musacchio, K.F. Jensen, S.L. Buchwald, Suzuki-Miyaura cross-coupling reactions in flow: multistep synthesis enabled by a microfluidic extraction, *Angew. Chem. Int. Ed.* 50 (2011) 5943–5946.
- [19] S.G. Newman, K.F. Jensen, The role of flow in green chemistry and engineering, *Green Chem.* 15 (2013) 1456–1472.
- [20] P. Plouffe, A. Macchi, D.M. Roberge, From batch to continuous chemical synthesis—a toolbox approach, *Org. Process Res. Dev.* 18 (2014) 1286–1294.
- [21] R.L. Hartman, J.P. McMullen, K.F. Jensen, Deciding whether to go with the flow: evaluating the merits of flow reactors for synthesis, *Angew. Chem. Int. Ed. Engl.* 50 (2011) 7502–7519.
- [22] B. Pieber, K. Gilmore, P.H. Seeberger, Integrated flow processing—challenges in continuous multistep synthesis, *J. Flow Chem.* (2017) 1–8.
- [23] A. Adamo, P.L. Heider, N. Weeranoppanant, K.F. Jensen, Membrane-based, liquid-liquid separator with integrated pressure control, *Ind. Eng. Chem. Res.* 52 (2013) 10802–10808.
- [24] D.X. Hu, M. O'Brien, S.V. Ley, Continuous multiple liquid-liquid separation: diazotization of amino acids in flow, *Org. Lett.* 14 (2012) 4246–4249.
- [25] H.R. Sahoo, J.G. Kralj, K.F. Jensen, Multistep continuous-flow microchemical synthesis involving multiple reactions and separations, *Angew. Chem. Int. Ed. Engl.* 46 (2007) 5704–5708.
- [26] R.J. Ingham, C. Battilocchio, D.E. Fitzpatrick, E. Sliwinski, J.M. Hawkins, S.V. Ley, A systems approach towards an intelligent and self-controlling platform for integrated continuous reaction sequences, *Angew. Chem. Int. Ed.* 54 (2015) 144–148.
- [27] K.F. Jensen, Flow chemistry—microreaction technology comes of age, *AlChE J.* 63 (2017) 858–869.
- [28] R.L. Hartman, J.R. Naber, N. Zaborenko, S.L. Buchwald, K.F. Jensen, Overcoming the challenges of solid bridging and constriction during Pd-Catalyzed C–N bond formation in microreactors, *Org. Process Res. Dev.* 14 (2010) 1347–1357.
- [29] J.R. Sedelmeier, S.V. Ley, I.R. Baxendale, M. Baumann, KMnO₄-mediated oxidation as a continuous flow process, *Org. Lett.* 12 (2010) 3618–3621.
- [30] D.L. Browne, B.J. Deadman, R. Ashe, I.R. Baxendale, S.V. Ley, Continuous flow processing of slurries: evaluation of an agitated cell reactor, *Org. Process Res. Dev.* 15 (2011) 693–697.
- [31] S.L. Poe, M.A. Cummings, M.P. Haaf, D.T. McQuade, Solving the clogging problem: precipitate-forming reactions in flow, *Angew. Chem. Int. Ed.* 45 (2006) 1544–1548.
- [32] T. Horie, M. Sumino, T. Tanaka, Y. Matsushita, T. Ichimura, J.-I. Yoshida, Photodimerization of maleic anhydride in a microreactor without clogging, *Org. Process Res. Dev.* 14 (2010) 405–410.
- [33] M.R. Chapman, M.H.T. Kwan, G. King, K.E. Jolley, M. Hussain, S. Hussain, I.E. Salama, C. González Niño, L.A. Thompson, M.E. Bayana, A.D. Clayton, B.N. Nguyen, N.J. Turner, N. Kapur, A.J. Blacker, Simple and versatile laboratory scale CSTR for multiphase continuous-flow chemistry and long residence times, *Org. Process Res. Dev.* 21 (2017) 1294–1301.
- [34] S. Falß, G. Tomaiuolo, A. Perazzo, P. Hodgson, P. Yaseneva, J. Zakrzewski, S. Guido, A. Lapkin, R. Woodward, R.E. Meadows, A continuous process for Buchwald-Hartwig amination at Micro-, Lab-, and Mesoscale using a novel reactor concept, *Org. Process Res. Dev.* 20 (2016) 558–567.
- [35] Y. Mo, K.F. Jensen, A miniature CSTR cascade for continuous flow of reactions containing solids, *React. Chem. Eng.* 1 (2016) 501–507.
- [36] R.A. Sheldon, Fundamentals of green chemistry: efficiency in reaction design, *Chem. Soc. Rev.* 41 (2012) 1437–1451.
- [37] C. Grondal, M. Jeanty, D. Enders, Organocatalytic cascade reactions as a new tool in total synthesis, *Nat. Chem.* 2 (2010) 167–178.
- [38] F. Galvanin, M. Sankar, S. Cattaneo, D. Bethell, V. Dua, G.J. Hutchings, A. Gavriilidis, On the development of kinetic models for solvent-free benzyl alcohol oxidation over a gold-palladium catalyst, *Chem. Eng. J.* 342 (2018) 196–210.
- [39] M. Morad, E. Nowicka, M. Douthwaite, S. Iqbal, P. Miedziak, J.K. Edwards, G.L. Brett, Q. He, D. Morgan, H. Alshammari, D. Bethell, D.W. Knight, M. Sankar, G.J. Hutchings, Multifunctional supported bimetallic catalysts for a cascade reaction with hydrogen auto transfer: synthesis of 4-phenylbutan-2-ones from 4-methoxybenzyl alcohols, *Catal. Sci. Technol.* 7 (2017) 1928–1936.
- [40] M.J. Climent, A. Corma, S. Iborra, M. Mifsud, A. Vely, New one-pot multistep process with multifunctional catalysts: decreasing the E factor in the synthesis of fine chemicals, *Green Chem.* 12 (2010) 99–107.
- [41] J.-I. Tateiwa, H. Horiuchi, K. Hashimoto, T. Yamauchi, S. Uemura, Cation-exchanged montmorillonite-catalyzed facile Friedel-Crafts alkylation of hydroxy and methoxy aromatics with 4-hydroxybutan-2-one to produce raspberry ketone and some pharmaceutically active compounds, *J. Org. Chem.* 59 (1994) 5901–5904.
- [42] S. Guadix-Montero, H. Alshammari, R. Dalebout, E. Nowicka, D.J. Morgan, G. Shaw, Q. He, M. Sankar, Deactivation studies of bimetallic AuPd nanoparticles supported on MgO during selective aerobic oxidation of alcohols, *Appl. Catal. A: General* 546 (2017) 58–66.
- [43] B. Ballarin, D. Barreca, E. Boanini, M.C. Cassani, P. Dambrosio, A. Massi, A. Mignani, D. Nanni, C. Parise, A. Zaghi, Supported gold nanoparticles for alcohols oxidation in continuous-flow heterogeneous systems, *ACS Sustain. Chem. Eng.* 5 (2017) 4746–4756.
- [44] H. Alex, N. Steinfeldt, K. Jähnisch, M. Bauer, S. Hübner, On the selective aerobic oxidation of benzyl alcohol with Pd/Au-nanoparticles in batch and flow, *Nano Rev.* 3 (2014) 99–110.
- [45] G. Wu, A. Constantinou, E. Cao, S. Kuhn, M. Morad, M. Sankar, D. Bethell, G.J. Hutchings, A. Gavriilidis, Continuous heterogeneous catalyzed oxidation of benzyl alcohol using a tube-in-tube membrane microreactor, *Ind. Eng. Chem. Res.* 54 (2015) 4183–4189.
- [46] N. Al-Rifai, F. Galvanin, M. Morad, E. Cao, S. Cattaneo, M. Sankar, V. Dua, G. Hutchings, A. Gavriilidis, Hydrodynamic effects on three phase micro-packed bed reactor performance – gold-palladium catalysed benzyl alcohol oxidation, *Chem. Eng. Sci.* 149 (2016) 129–142.
- [47] N. Al-Rifai, P.J. Miedziak, M. Morad, M. Sankar, C. Waldron, S. Cattaneo, E. Cao, S. Pattison, D. Morgan, D. Bethell, G.J. Hutchings, A. Gavriilidis, Deactivation behavior of supported gold palladium nanoalloy catalysts during the selective oxidation of benzyl alcohol in a micropacked bed reactor, *Ind. Eng. Chem. Res.* 56 (2017) 12984–12993.
- [48] E. Cao, G. Brett, P.J. Miedziak, J.M. Douthwaite, S. Barras, P.F. McMillan, G.J. Hutchings, A. Gavriilidis, A micropacked-bed multi-reactor system with in situ Raman analysis for catalyst evaluation, *Catal. Today* 283 (2017) 195–201.
- [49] E. Cao, M. Sankar, S. Firth, K.F. Lam, D. Bethell, D.K. Knight, G.J. Hutchings, P.F. McMillan, A. Gavriilidis, Reaction and Raman spectroscopic studies of alcohol

- oxidation on gold-palladium catalysts in microstructured reactors, *Chem. Eng. J.* 167 (2011) 734–743.
- [50] E. Cao, M. Sankar, E. Nowicka, Q. He, M. Morad, P.J. Miedziak, S.H. Taylor, D.W. Knight, D. Bethell, C.J. Kiely, A. Gavriilidis, G.J. Hutchings, Selective suppression of disproportionation reaction in solvent-less benzyl alcohol oxidation catalysed by supported Au–Pd nanoparticles, *Catal. Today* 203 (2013) 146–152.
- [51] M. Morad, M. Sankar, E. Cao, E. Nowicka, T.E. Davies, P.J. Miedziak, D.J. Morgan, D.W. Knight, D. Bethell, A. Gavriilidis, G.J. Hutchings, Solvent-free aerobic oxidation of alcohols using supported gold palladium nanoalloys prepared by a modified impregnation method, *Catal. Sci. Technol.* 4 (2014) 3120–3128.
- [52] Y. He, A. Jawad, X. Li, M. Atanga, F. Rezaei, A.A. Rownaghi, Direct aldol and nitroaldol condensation in an aminosilane-grafted Si/Zr/Ti composite hollow fiber as a heterogeneous catalyst and continuous-flow reactor, *J. Catal.* 341 (2016) 149–159.
- [53] S. Wang, K. Goulas, E. Iglesia, Condensation and esterification reactions of alkanals, alkanones, and alkanols on TiO₂: elementary steps, site requirements, and synergistic effects of bifunctional strategies, *J. Catal.* 340 (2016) 302–320.
- [54] A. Fischer, P. Makowski, J.O. Müller, M. Antonietti, A. Thomas, F. Goettmann, High-surface-area TiO₂ and TiN as catalysts for the C–C coupling of alcohols and ketones, *ChemSusChem* 1 (2008) 444–449.
- [55] J.E. Rekoske, M.A. Barteau, Kinetics, selectivity, and deactivation in the aldol condensation of acetaldehyde on anatase titanium dioxide, *Ind. Eng. Chem. Res.* 50 (2011) 41–51.
- [56] I. Paterová, E. Vyskočilová, L. Červený, Two-step preparation of benzylacetone, *Top. Catal.* 55 (2012) 873–879.
- [57] N. Linares, C. Moreno-Marrodan, P. Barbaro, PdNP@ titanate nanotubes as effective catalyst for continuous-flow partial hydrogenation reactions, *ChemCatChem* 8 (2016) 1001–1011.
- [58] N. Linares, S. Hartmann, A. Galarneau, P. Barbaro, Continuous partial hydrogenation reactions by Pd@ unconventional bimodal porous Titania monolith catalysts, *ACS Catal.* 2 (2012) 2194–2198.
- [59] M. O'Brien, N. Taylor, A. Polyzos, I.R. Baxendale, S.V. Ley, Hydrogenation in flow: homogeneous and heterogeneous catalysis using Teflon AF-2400 to effect gas-liquid contact at elevated pressure, *Chem. Sci.* 2 (2011) 1250–1257.
- [60] C. Liebner, J. Fischer, S. Heinrich, T. Lange, H. Hieronymus, E. Klemm, Are micro reactors inherently safe? An investigation of gas phase explosion propagation limits on ethene mixtures, *Process Saf. Environ. Prot.* 90 (2012) 77–82.
- [61] N. Kockmann, P. Theneß, C. Fleischer-Trebes, G. Laudadio, T. Noel, Safety assessment in development and operation of modular continuous-flow processes, *React. Chem. Eng.* 2 (2017) 258–280.